Inframatics, 2023, 4, 1-11
https://www.scirp.org/journal/inframatics
ISSN Online: 2160-5874
ISSN Print: 2160-5866

Migration of Source Locations and Arrival Orientations for Infrasound Excitation in the Lützow-Holm Bay, Antarctica: January - April 2017

Takahiko Murayama[1*], Masaki Kanao[2], Masa-Yuki Yamamoto[3]

[1]Japan Weather Association, Tokyo, Japan
[2]National Institute of Polar Research, Research Organization of Information and Systems, Tokyo, Japan
[3]School of Systems Engineering, Kochi University of Technology, Kochi, Japan
Email: *murayama@jwa.or.jp, kanao@nipr.ac.jp, yamamoto.masa-yuki@kochi-tech.ac.jp

How to cite this paper: Murayama, T., Kanao, M. and Yamamoto, M.-Y. (2023) Migration of Source Locations and Arrival Orientations for Infrasound Excitation in the Lützow-Holm Bay, Antarctica: January - April 2017. *Inframatics*, **4**, 1-11.
https://doi.org/10.4236/inframatics.2023.41001

Received: September 14, 2023
Accepted: October 24, 2023
Published: October 27, 2023

Abstract

Predominant phenomenon of the migration in source locations and arrival orientations for infrasound excitation was clearly identified by using a combination of two arrays deployed at the coast of the Lützow-Holm Bay (LHB), Antarctica during the period from January to April in 2017. A few tens of infrasound source locations were determined in several individual days during four months in 2017. These identified source locations appeared to be migrated from the north-east direction to the north-west direction from January to April in 2017, the evidence assumed to be caused by time-offset effects between katabatic winds from continental ice sheet and the microbaroms from the LHB, based on comparison with oceanic wave heights around Antarctica and Southern Indian Ocean calculated by the wave model (WAM). The latter source locations in the north-west direction were also considered to be related with the sea-ice dynamics involving collapse and/or discharge from the LHB to the Ocean by comparison with MODIS satellite image.

Keywords

Infrasound, Array Analyses, Antarctica, Katabatic Winds, Microbaroms, Sea-Ice Dynamics

1. Introduction

In the polar regions including Antarctica, atmospheric pressure variations are affected by mutual interaction between the atmosphere and surrounding environment, such as oceans, cryosphere, and the surface of solid earth. Origin of the sources in mutual interaction appearing in atmospheric pressure can be measured by infrasound sensors deployed in the polar regions. Infrasound is categorized as a sub-audible pressure wave with frequency content from the cut-off of a sound (3.21 mHz, for a 15˚C atmosphere) to the lowest of the human audible band (20 Hz) and propagate thousands of kilometers along the Earth's surface by considerable excitation energy [1]. There have been many observations of the infrasound excitation by a few generating sources in the world; volcanic eruptions, oceanic swells, large earthquakes, aircrafts, thunder and sprites, fireballs, meteoroid, reentry of artificial vehicles and aurora activities, etc. [2] [3] [4] [5] [6].

In Antarctica, the infrasound measurements started in April 2008 using a single sensor at Syowa Station (SYO; 69.0S, 39.6E) in the Lützow-Holm Bay (LHB) (**Figure 1**). In the austral summer of 2014, two infrasound arrays were newly deployed both on the outcrop site at SYO and continental ice sheet (S16 point)

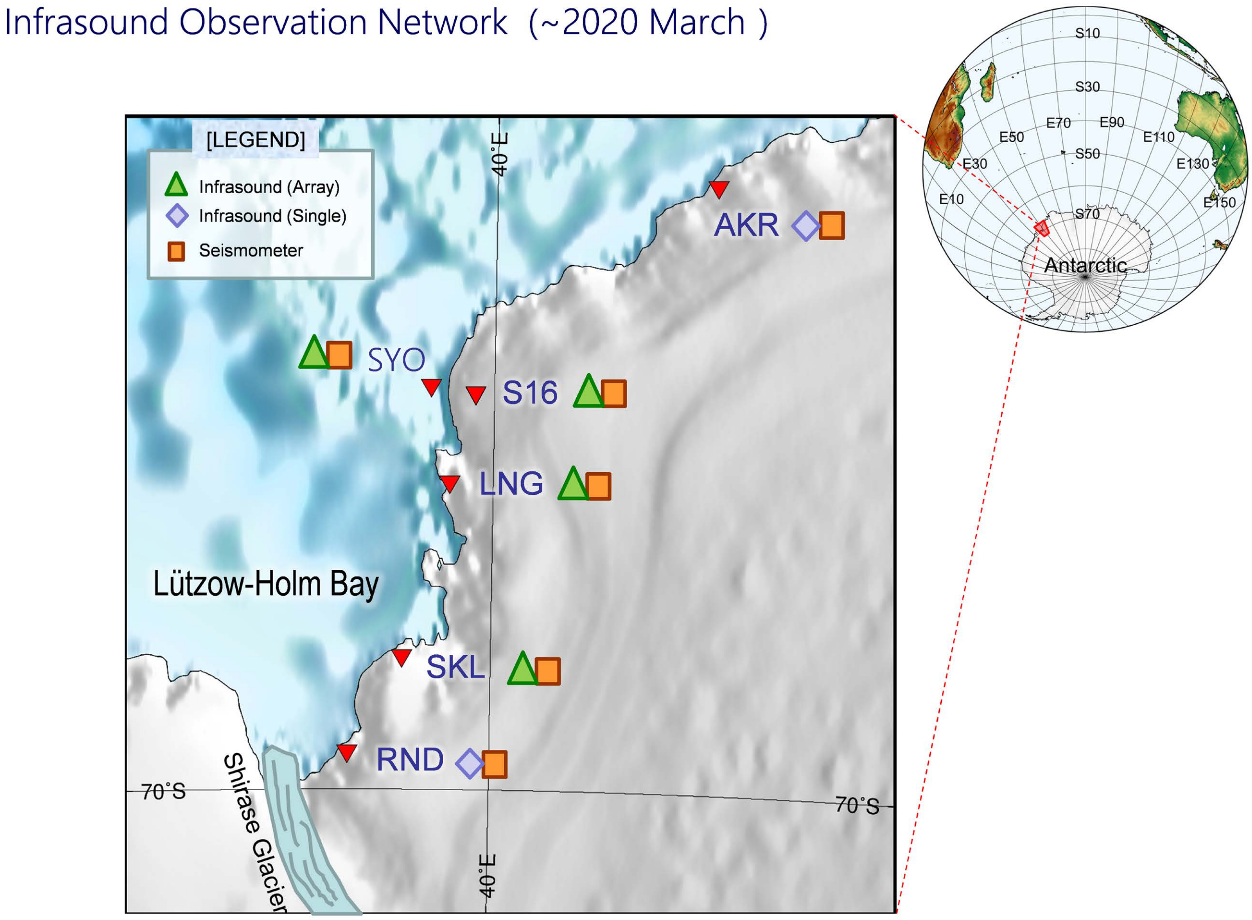

Figure 1. Locations of infrasound observation network in the Lützow-Holm Bay (LHB) region, Antarctica as of 2017. Array stations of infrasound (green triangles), single stations of infrasound (blue diamond) and broadband seismometers (orange squares) are shown. Abbreviation of the local names are as follows: SYO: Syowa Station, AKR: Akarui Misaki, LNG: Langhovde, SKL: Skallen, RND: Rundvagshetta.

near the eastern coast of the LHB, in addition to several outcrop stations (Langhovde, Skallen and Rundvagshetta) by using isolated single sensors (**Figure 1**) [7]. From the data obtained by the SYO array, long-term variations for eleven years in 2008-2019 were already reported [8], treating their frequency contents and source orientations of the microbaroms from the Southern Indian Ocean. The long-term variability of the microbaroms could be new information on estimating ocean climate trends in the costal margin of the Antarctic.

By using a combination of the two arrays at SYO and S16 deployed in LHB, three infrasound sources were identified during the 2015 winter season, providing the source locations along the coast, within the sea-ice area of the LHB and surrounding SYO, respectively [9]. In addition, a longer-term variability of the source locations of infrasound excitation for eight months in January-August 2015 was investigated by utilizing the same two arrays [10]. Considerable source mechanisms of these detected events were estimated involving surface environmental change, in particular cryosphere dynamics surrounding the LHB, associated with discharge of the fast-sea-ice in April 2015. In April 2016, moreover, succeeding analyses by using the same two arrays revealed a relationship between the source locations in the LHB direction and the occurrence of sea-ice-discharge event at the month [11].

In this paper, in addition to these previous studies at the target region of LHB, time-space variations of the source locations for the infrasound excitation from January to April in 2017 was studied by using a combination of the same two arrays deployed along the coast of LHB, in term of relationship between surface environment such as cryosphere dynamics and ocean climate variability around the LHB and the Southern Indian Ocean. By using the arrays, we can further investigate the characteristics of low frequency sounds in Antarctica, its sensitivity to the environment and weather forecast, as well as its potential application in the study of seismology and climate change in southern high latitudes.

2. Array Analyses

A total of nine infrasound sensors have been observed along the eastern coast of the LHB since January 2013 [7]. Two triangle array alignments with different diameters were established at SYO (with a 100 m spacing triangle), and a vicinity of the S16 point over the ice sheet (1 km space triangle) where 15 km eastward from the SYO array (**Figure 2**). The different configuration of the two arrays was adopted to localize the detected signals efficiently by recognizing identical wavelengths with corresponding frequencies for each array size. The Chaparral Physics micro barometer (Model 25, detectable frequency of 0.1 - 200 Hz) has been utilized in these stations. Moreover, the hose arrays were aligned to reduce wind noises by adopting the mechanical low-pass filtering [12] [13]. Multiply connected porous hoses were also used at the SYO array; in contrast, a single array configuration was used at other stations to make simplify their logistical installations. These porous hoses were buried beneath the mounds of stones or snow-ice collected from around the observation sites to reduce the vibration effect of the winds. Detail configuration of these observation systems was described in [7].

To estimate the propagation directions and locations of the infrasound sources, a multiple step approach was utilized; the first step was to compile a catalog for each array using a progressive multi-channel correlation algorithm (PMCC) [14] [15]; the second step was by using the two bulletins of the arrays (SYO and S16). A systematic flow of the array analysis is as follows; 1) search the pairs of signals within ±80 s of detected time difference on the basis of the bulletin dataset for both arrays on the basis of the distance of two arrays is about 20 km; 2) calculate the cross point by using a spherical triangle method based on propagation direction and apparent velocities for each array; 3) set the candidate origin as grids around the cross point within ±5 deg range, followed by calculating averaged origin time and select the most probable grid; 4) evaluate calculated apparent velocities (V) within the range of (0.28 m/s ≤ V ≤ 0.36 m/s) for both the arrays, respectively.

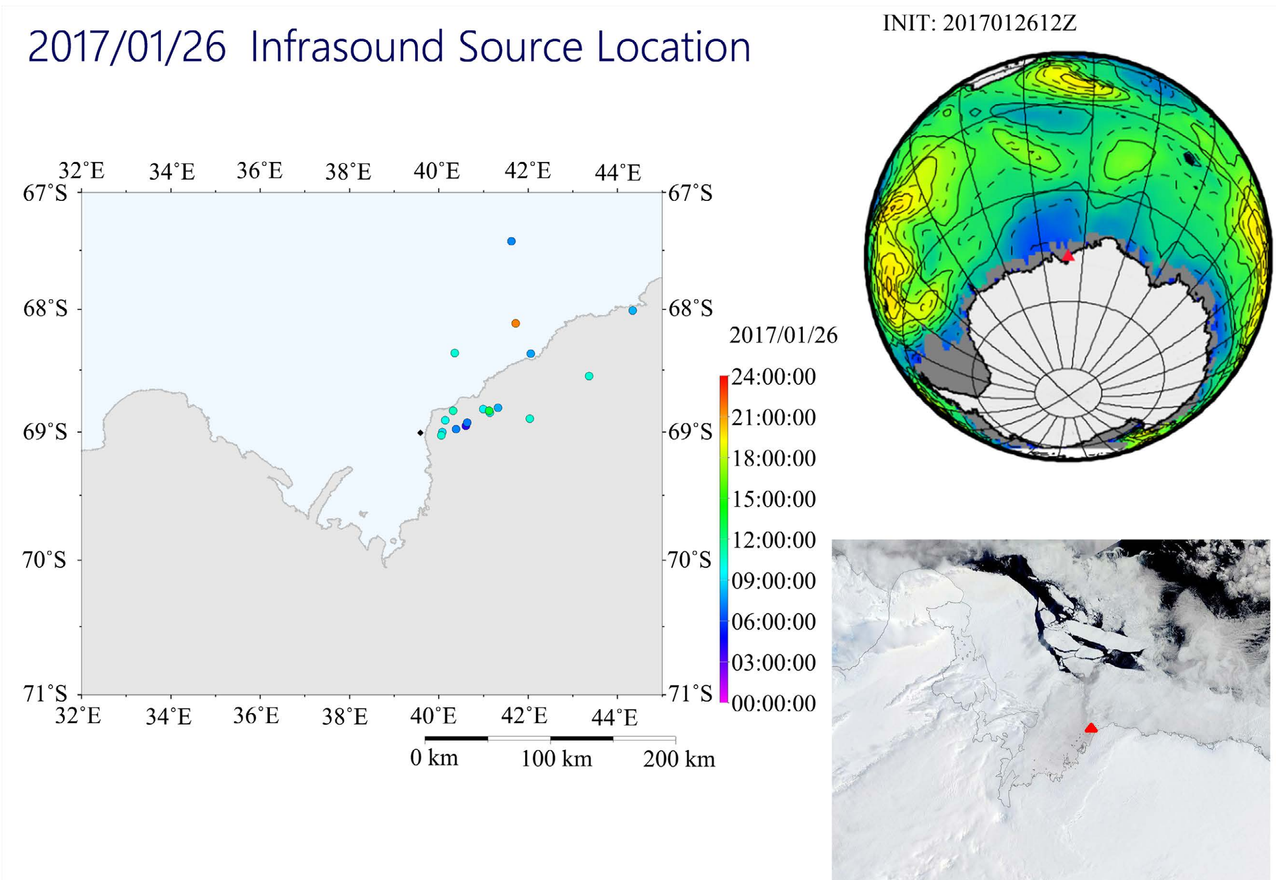

Figure 2. (left) Source locations of infrasound excitation estimated by using two arrays of SYO and S16 (shown by black solid diamonds in the panel) in the LHB on January 26, 2017. The source locations are colored according to the time from the beginning of the day. (upper right) Distribution of oceanic wave heights around Antarctica and Southern Indian Ocean calculated by the WAM model [16] [17] [18] on the same day. (lower right) MODIS satellite images around the LHB on January 26, 2017. SYO is indicated by red triangle.

3. Results and Discussion

Source locations and arrival orientations for the infrasound excitation were investigated by using a combination of the two arrays (SYO and S16) deployed at the coast of LHB during the period from January to April in 2017. A few tens of infrasound source locations were determined in several different days during the four months. A total of six examples of the detected source locations by the array analyses will be demonstrated in this section. The results from array analyses by the PMCC algorithm are shown in **Figures 2-6**.

Figure 2 represents the source locations of the infrasound excitation estimated by using two arrays in LHB for the day on January 26, 2017. The source locations are colored according to the time from the beginning of the day. Majority of the detected events were determined in the north-east direction from the SYO array. Distribution of the global oceanic wave heights around East Antarctic continent and the Southern Indian Ocean calculated by the WAM Cycle 4 model [16] [17] [18] on the same day is also shown in the figure. The Ocean Wave Hindcast Database was provided by the Japan Weather Association

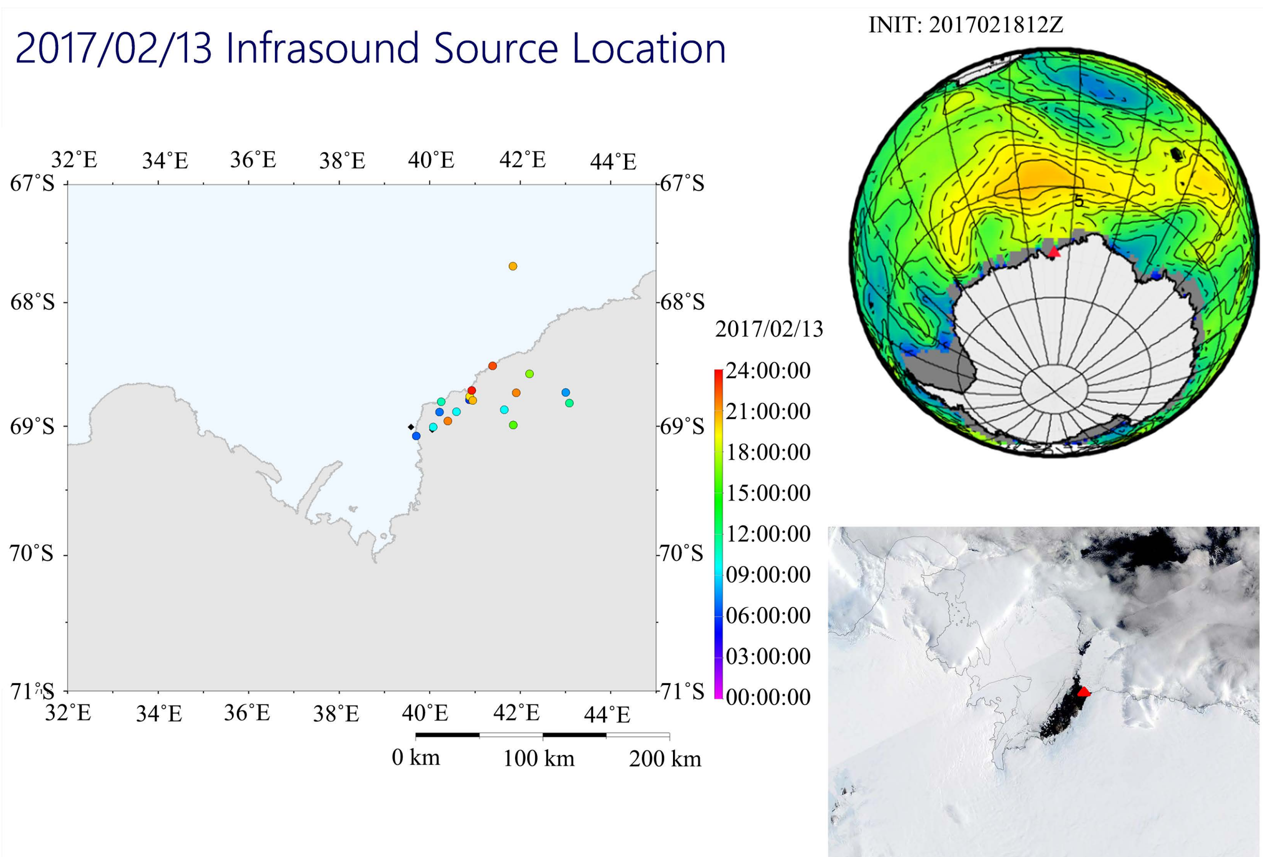

Figure 3. (left) Source locations of infrasound excitation estimated by using two arrays of SYO and S16 (shown by black solid diamonds in the panel) in the LHB on February 13, 2017. The source locations are colored according to the time from the beginning of the day. (upper right) Distribution of oceanic wave heights around Antarctica and Southern Indian Ocean calculated by the WAM model [16] [17] [18] on February 18, 2017. (lower right) MODIS satellite images around the LHB on February 13, 2017. SYO is indicated by red triangle.

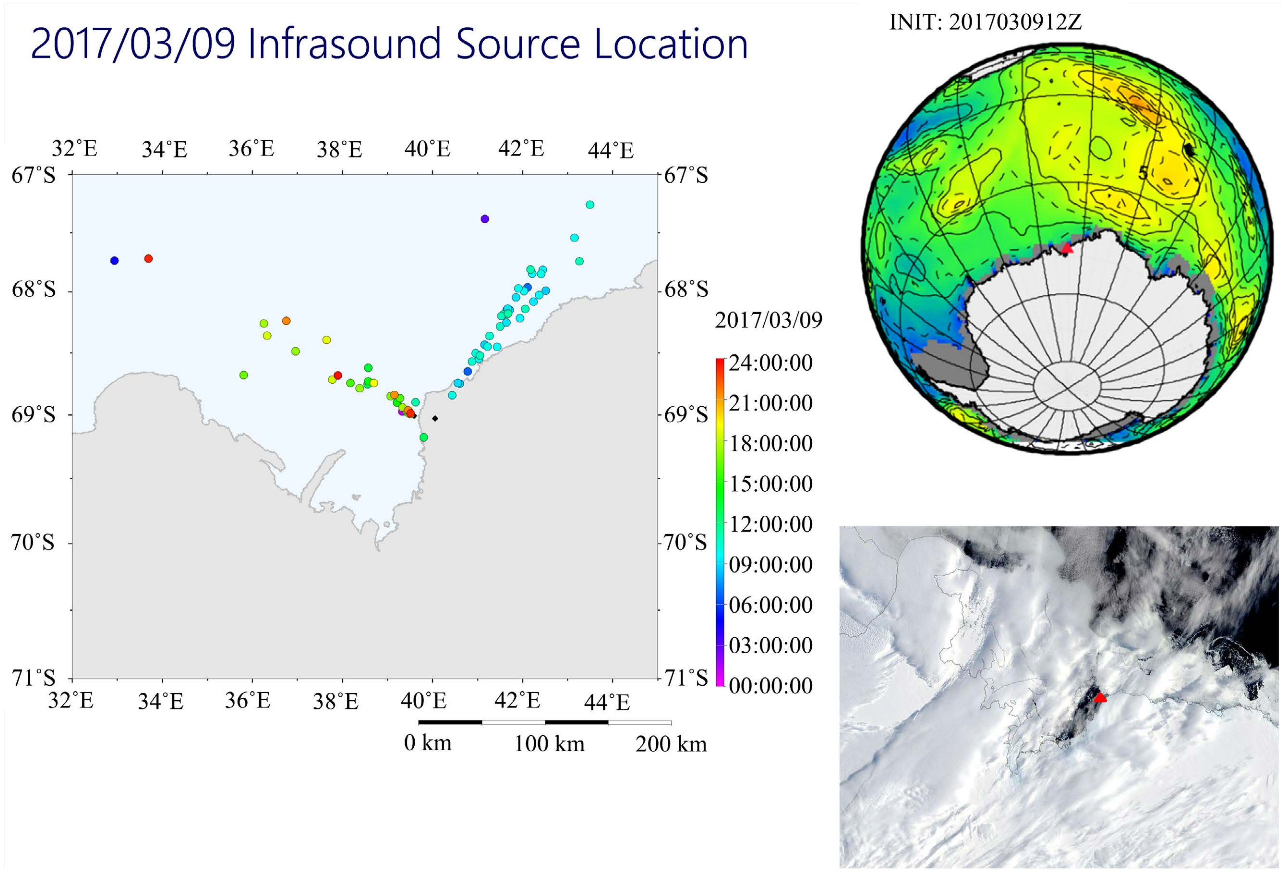

Figure 4. (left) Source locations of infrasound excitation estimated by using two arrays of SYO and S16 (shown by black solid diamonds in the panel) in the LHB on March 9, 2017. The source locations are colored according to the time from the beginning of the day. (upper right) Distribution of oceanic wave heights around Antarctica and Southern Indian Ocean calculated by the WAM model [16] [17] [18] on the same day. (lower right) MODIS satellite images around the LHB on March 9, 2017. SYO is indicated by red triangle.

(https://www.jwa.or.jp/service/transport-support/waves-03/). As the input wind fields in the calculation, the the National Centers for Environmental Prediction - National Center for Atmospheric Research (NCEP–NCAR) reanalysis data was utilized. Besides, the MODIS satellite images (provided by NASA) which give cryosphere information at the target area around LHB in the same day on January 26, 2017, are also inserted in the figure. It cannot identify the existence of large storms in the Southern Indian Ocean at the day; therefore, the determined orientations for the most infrasound events on the day could probably be associated with the katabatic winds from continental ice sheet in the north-east direction to the LHB direction. As there were no events determined inside the LHB (*i.e.*, the north-west direction from the SYO array), dynamics of the cryosphere in particular involving sea-ice movements did not generate the infrasound events at the day, in spite of the pre-existed sea-ice cracks and separated fast-sea-ice pieces are clearly recognized in the MODIS image.

By the similar representation as in **Figure 2**, source locations of the infrasound excitation estimated by a combination of the two arrays at SYO and S16,

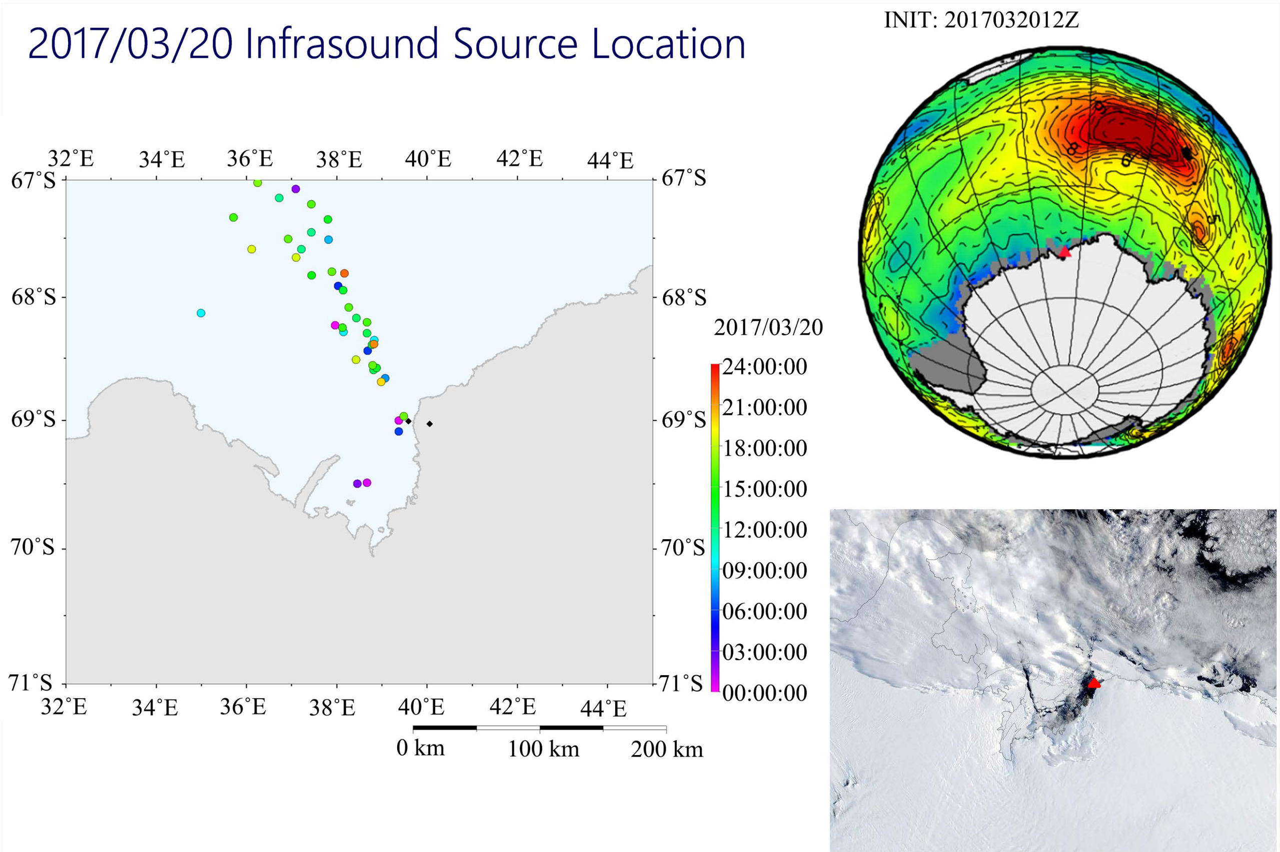

Figure 5. (left) Source locations of infrasound excitation estimated by using two arrays of SYO and S16 (shown by black solid diamonds in the panel) in the LHB on March 20, 2017. The source locations are colored according to the time from the beginning of the day. (upper right) Distribution of oceanic wave heights around Antarctica and Southern Indian Ocean calculated by the WAM model [16] [17] [18] on the same day. (lower right) MODIS satellite images around the LHB on March 20, 2017. SYO is indicated by red triangle.

distribution of oceanic wave heights around Antarctica and Southern Indian Ocean calculated by the WAM model, the MODIS satellite images around the LHB are shown in **Figures 3-6**, for the different days on February 18, March 9, March 20, and April 16, 2017, respectively. Predominant migration phenomenon in the source locations and arrival orientations for the infrasound excitation were clearly identified by the array analyses from January to April in 2017, as clearly recognized in these figures. The identified source locations of the infrasound events appeared to be migrated from the north-east direction to the north-west direction from January to April in 2017, which could be assumed to be caused by the time-offset effects between the katabatic winds from continental ice sheet and the microbaroms originated from the LHB, based on comparison with oceanic wave height around Antarctica and southern Indian Ocean calculated by the WAM model.

The latter sources of infrasound exciton from the north-west direction were also considered to be related with the sea-ice dynamics involving its collapse and/or discharge from the LHB to the Sothern Indian Ocean by comparison with the MODIS satellite images. The infrasound excitation could be generated

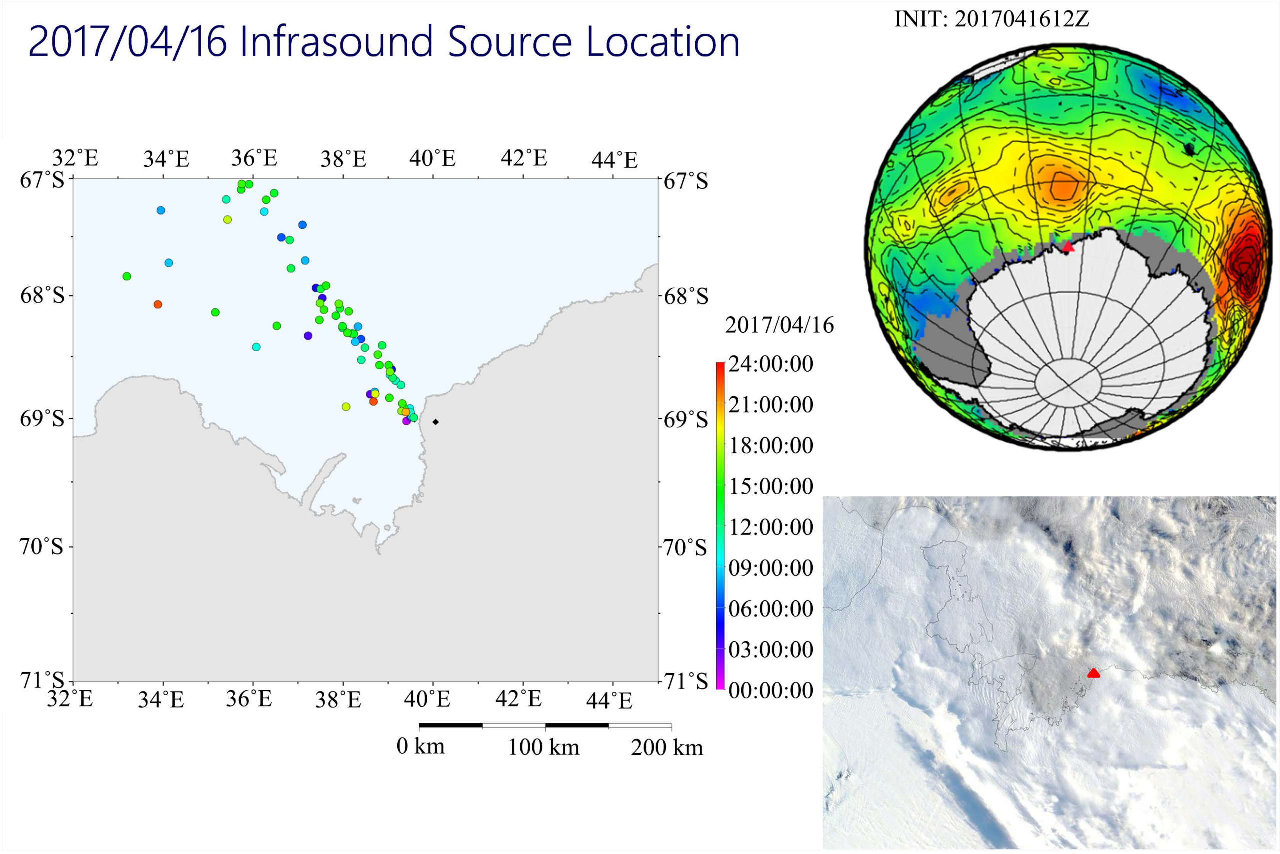

Figure 6. (left) Source locations of infrasound excitation estimated by using two arrays of SYO and S16 (shown by black solid diamonds in the panel) in the LHB on April 16, 2017. The source locations are colored according to the time from the beginning of the day. (upper right) Distribution of oceanic wave heights around Antarctica and Southern Indian Ocean calculated by the WAM model [16] [17] [18] on the same day. (lower right) MODIS satellite images around the LHB on April 16, 2017. SYO is indicated by red triangle.

when the energy of microbaroms were significant such as the period for the visits of large storms near the offshore of LHB. This interpretation could also be confirmed by the oceanic wave heights by the WAM model at the days on March 20, and April 16. The source orientations determined in the north-west direction were the similar pattern to the same two array results of the LHB in April 2015 [10] and in April 2016 [11], respectively. This evidence can be supported by the occurrence of cryosphere dynamics such as the discharge of a large volume of sea-ice at the months in the LHB.

Regarding the source locations on March 9, two directions (*i.e.*, the north-east and the north-west) of the infrasound excitation were determined, when it was the boundary season from the katabatic dominated periods to the microbaroms/sea-ice related events dominated ones. When checking the day in more detail, infrasound events from the north-east directions were found to be concentrated in the morning in a day, when it was the dominant time zone for the katabatic winds in the LHB area. In contrast, the infrasound events in the north-west directions had assumed to be occurred in the afternoon and later time zones, when the katabatic winds generally became small energy and amplitudes. It is also mentioned that the katabatic winds were generally recognized that their energy/appearance are large at the austral fall seasons in the Antarctic, which is consistent with this result by infrasound array analyses.

Involving the effects of the oceanic swells from the Bay, moreover, the microbaroms could be varied significantly both in the amplitude and frequency contents. These characteristic variations were affected by the local atmospheric conditions in the vicinity of the studied area [19]. Infrasound signals under 3 Hz frequency content were supposed to contain in some extent the microbaroms which can be excited by the storms during whole seasons particular in austral winter. By conducting this study, configuration for the infrasound arrays deployed in the LHB had efficiently been operating, and the arrays provided useful information on the arrival directions of infrasound excitation sources associated with surface environmental variations. Moreover, the influence of the downslope wind of the continental ice sheet and the time difference between the microbaroms and the sound source migration of the LHB on the results, as well as the possible physical mechanism, can be further explored more detail.

Finally, precise locations of the infrasound sources might be compared with information obtained by other geophysical investigations. For example, recently [20] conducted simultaneous observations by both the seismic and infrasound sensors at the Bowdoin Glacier in Greenland. They found ground validate infrasound sources very precisely by using time-lapse cameras and better-localized sources due to their small size. In terms of the importance of this study for monitoring climate change and environment in Antarctica, we suggest the directions for further research in the future, such as comparative analysis with other observational data, as well as the longer time span observations in the surrounding Antarctic regions. The oceanic-atmospheric coupling effects on the infrasound excitation were well explained by the relationship within the complex Earth system in the polar environment. In this aspect, long-term monitoring of the infrasound excitation in the Antarctic could be a useful tool for detecting the environmental variations within the climate change which is now going on over the Earth.

4. Summary

This paper reported a predominant migration phenomenon in the source locations for the infrasound excitation identified by using two arrays deployed in the LHB of Antarctica during four months from January to April in 2017. A few tens of infrasound sources were determined at five individual days, and the source locations had shifted from the north-east direction to the north-west direction, which could be caused by the time-offset effects between the katabatic winds and the microbaroms from the LHB, based on oceanic wave heights around Antarctica by the WAM model. In addition, the latter sources from the north-west direction could be involved in the sea-ice relating dynamics in the Bay based on a comparison with the MODIS satellite images.

Acknowledgements

The authors express their sincere appreciation to the collaborators regarding infrasound observations in Antarctica, for the members of the Japanese Antarctic Research Expeditions (JARE). The authors also acknowledge the National Aeronautics and Space Administration (NASA) for the utilization of MODIS images. They also thank the NCEP reanalysis data provided by the NOAA/OAR/ESRL PSD, Boulder, Colorado, USA, from their Web site at http://www.cdc.noaa.gov/. Finally, the authors acknowledge the Ocean Wave Hindcast Database provided by the Japan Weather Association (https://www.jwa.or.jp/service/transport-support/waves-03/).

Conflicts of Interest

The authors declare no conflicts of interest regarding the publication of this paper.

References

[1] Hedlin, M., Garces, M., Bass, H., Hayward, C., Herrin, G., Olson, J.V. and Wilson, C. (2002) Listening to the Secret Sounds of Earth's Atmosphere. *Eos*, *Transactions American Geophysical Union*, **83**, 557-565. https://doi.org/10.1029/2002EO000383

[2] Arai, N., Iwakuni, M., Watada, S., Imanishi, Y., Murayama, T. and Nogami, M. (2011) Atmospheric Boundary Waves Excited by the Tsunami Generation Related to the 2011 Great Tohoku-Oki Earthquake. *Geophysical Research Letters*, **38**, L00G18. https://doi.org/10.1029/2011GL049146

[3] Matoza, R.S., Hedlin, M.A.H. and Garces, M.A. (2007) An Infrasound Array Study of Mount St. Helens. *Journal of Volcanology and Geothermal Research*, **160**, 249-262. https://doi.org/10.1016/j.jvolgeores.2006.10.006

[4] Arrowsmith, S.J., ReVelle, D.O., Edwards, W.N. and Brown, P. (2008) Global Infrasonic Signals from Three Large Bolides. *Earth*, *Moon and Planets*, **102**, 357-363. https://doi.org/10.1007/s11038-007-9205-z

[5] Le Pichon, A., Blanc, E. and Drob, D. (2005) Probing High-Altitude Winds Using Infrasound. *Journal of Geophysical Research*: *Atmospheres*, **110**, D20104. https://doi.org/10.1029/2005JD006020

[6] Wilson, C.R. (1969) Auroral Infrasonic Waves. *Journal of Geophysical Research*, **747**, 1812-1836. https://doi.org/10.1029/JA074i007p01812

[7] Murayama, T., Kanao, M., Yamamoto, M.Y., Ishihara, Y., Matshushima, T. and Kakinami, Y. (2015) Infrasound Array Observations in the Lützow-Holm Bay Region, East Antarctica. *Polar Science*, **9**, 35-50. https://doi.org/10.1016/j.polar.2014.07.005

[8] Ishihara, Y., Murayama, T., Yamamoto, M.Y., Matsushima, T. and Kanao, M. (2020) Infrasound Observation at Japanese Antarctic Station Syowa: 11 Years Observations and Results. *Polar Data Journal*, **4**, 45-54.

[9] Murayama, T., Kanao, M., Yamamoto, M.Y. and Ishihara, Y. (2017) Infrasound Signals and Their Source Location Inferred from Array Deployment in the Lützow-Holm Bay Region, East Antarctica: January-June 2015. *International Journal of Geosciences*, **8**, 181-188. https://doi.org/10.4236/ijg.2017.82007

[10] Murayama, T., Kanao, M., Yamamoto, M.Y., Ishihara, Y., Matshushima, T., Kakinami,

Y., Okada, K., Miyamachi, H., Nakamoto, M., Takeuchi, Y. and Toda, S. (2017b) Time-Space Variations of Infrasound Sources Related to Environmental Dynamics around the Lutzow-Holm Bay, East Antarctica. *Polar Science*, **14**, 39-48. https://doi.org/10.1016/j.polar.2017.10.001

[11] Murayama, T., Kanao, M. and Yamamoto, M.Y. (2018) Characteristic Infrasound Events Associated with Sea-Ice Discharges in the Lützow-Holm Bay of Antarctica: April 2016. In: Kanao, M., Toyokuni, G. and Yamamoto, M.Y., Eds., *Antarctica—A Key to Global Change*, IntechOpen, London, 1-10. https://doi.org/10.5772/intechopen.83023

[12] Walker, K.T. and Hedlin, M.A.H. (2010) A Review of Wind-Noise Reduction Methodologies. In: Pichon, A.L., Blanc, E. and Hauchecorne, A., Eds., *Infrasound Monitoring for Atmospheric Studies*, Springer, Dordrecht, 141-182. https://doi.org/10.1007/978-1-4020-9508-5

[13] Hedlin, M. and Alcoverro, B. (2005) The Use of Impedance Matching Capillaries for Reducing Resonance in Rosette Infrasonic Spatial Filters. *The Journal of the Acoustical Society of America*, **117**, 1880-1888. https://doi.org/10.1121/1.1760778

[14] Cansi, Y. (1995) An Automatic Seismic Event Processing for Detection and Location: The P.M.C.C. Method. *Geophysical Research Letters*, **22**, 1021-1024. https://doi.org/10.1029/95GL00468

[15] Cansi, Y. and Klinger, Y. (1997) An Automated Data Processing Method for Mini-Arrays, CSEM/EMSC European-Mediterranean Seismological Centre. *News Letters*, **11**, 1021-1024.

[16] The Wamdi Group (1988) The WAM Model—A Third Generation Ocean Wave Prediction Model. *Journal of Physical Oceanography*, **18**, 1775-1810. https://doi.org/10.1175/1520-0485(1988)018<1775:TWMTGO>2.0.CO;2

[17] Günther, H., Hasselmann, S. and Janssen, P.A.E.M. (1992) The WAM Model Cycle 4.0. User Manual. Technical Report No. 4, Deutsches Klimarechenzentrum, Hamburg.

[18] Komen, G.J., Cavaleri, L., Donelan, M., Hasselmann, K., Hasselmann, S. and Janssen, P.A.E.M. (1994) Dynamics and Modeling of Ocean Waves. Cambridge University Press, Cambridge. https://doi.org/10.1017/CBO9780511628955

[19] Kanao, M., Maggi, A., Ishihara, Y., Yamamoto, M.Y., Nawa, K., Yamada, A., Wilson, T., Himeno, T., Toyokuni, G., Tsuboi, S., Tono, Y. and Anderson, K. (2012) Interaction of Seismic Waves between Atmosphere-Ocean-Cryosphere and Geosphere in Polar Region. In: Kanao, M., Ed., *Seismic Waves—Research and Analysis*, InTech. Publisher, Rijeka, 1-20. https://doi.org/10.5772/23410

[20] Podolskiy, E.A., Genco, R., Sugiyama, S., Walter, F., Funk, M., Minowa, M., Tsutaki, S. and Ripepe, M. (2017) Seismic and Infrasound Monitoring of Bowdoin Glacier, Greenland. *Low Temperature Science*, **75**, 15-36.